

# A Study of Propagation of Spherically Expanding and Counterflow Laminar Flames Using Direct Measurements and Numerical Simulations

Jagannath Jayachandran,<sup>1</sup> Alexandre Lefebvre,<sup>2</sup> Runhua Zhao,<sup>1</sup> Fabien Halter,<sup>3</sup>  
Emilien Varea,<sup>2</sup> Bruno Renou,<sup>2</sup> Fokion N. Egolfopoulos<sup>1</sup>

<sup>1</sup>*Department of Aerospace and Mechanical Engineering  
University of Southern California, Los Angeles, California 90089-1453, USA*

<sup>2</sup>*CORIA UMR 6614 CNRS  
INSA de Rouen, 76801 Saint Etienne du Rouvray, France*

<sup>3</sup>*Laboratoire PRISME, Université d'Orléans, 45072 Orléans, France*

## Corresponding Author:

Jagannath Jayachandran  
Department of Aerospace and Mechanical Engineering,  
University of Southern California  
Los Angeles, California 90089-1453, USA  
Phone: 213-740-4332  
Fax: 213-740-8071  
Email: jjayacha@usc.edu

Colloquium Topic Area: Laminar Flames

Manuscript PROCI-D-13-00729

Total length: 5761 words  
Main text: 3359 words (MSWord 2010 word count)  
References: (42 references + 2) x (2.3 line/reference) x (7.6 words/line) = 770 words  
Figure 1: [122 mm + 10 mm] x 2.2 words/mm x 1 column + (38 words in caption) = 329 words  
Figure 2: [122 mm + 10 mm] x 2.2 words/mm x 1 column + (38 words in caption) = 329 words  
Figure 3: [37 mm + 10 mm] x 2.2 words/mm x 2 column + (24 words in caption) = 231 words  
Figure 4: [83 mm + 10 mm] x 2.2 words/mm x 2 column + (61 words in caption) = 471 words  
Figure 5: [42 mm + 10 mm] x 2.2 words/mm x 2 column + (43 words in caption) = 272 words  
Figure (total): 1632 words

Accepted for presentation at the 35<sup>th</sup> International Symposium on Combustion, San Francisco, California, USA, August 3 – 8, 2014.

# A Study of Propagation of Spherically Expanding and Counterflow Laminar Flames Using Direct Measurements and Numerical Simulations

Jagannath Jayachadran,<sup>1</sup> Alexandre Lefebvre,<sup>2</sup> Runhua Zhao,<sup>1</sup> Fabien Halter,<sup>3</sup>  
Emilien Varea,<sup>2</sup> Bruno Renou,<sup>2</sup> Fokion N. Egolfopoulos<sup>1</sup>

<sup>1</sup>*Department of Aerospace and Mechanical Engineering  
University of Southern California, Los Angeles, California 90089-1453, USA*

<sup>2</sup>*CORIA UMR 6614 CNRS  
INSA de Rouen, 76801 Saint Etienne du Rouvray, France*

<sup>3</sup>*Laboratoire PRISME, Université d'Orléans, 45072 Orléans, France*

## Abstract

Spherically expanding and counterflow flame configurations are used extensively to determine laminar flame speeds. Significant advances have been made over the years with both the theoretical and experimental aspects of these standard experiments. However, discrepancies still persist in reported laminar flame speed data raising the question of accuracy and consistency. Among the probable reasons that the discrepancy among reported data is that laminar flame speed is a derived and not a directly measured physical quantity, leaving thus room for interpretations that typically introduce additional uncertainties. In the present investigation, a combined experimental and modeling study was carried out for first time in both configurations. Ethylene and *n*-heptane flames were considered and the flow velocities were measured using particle image velocimetry in both spherically expanding and counterflow flames. The accuracy and consistency of the results were assessed by comparing directly measured and directly computed physical properties. It was shown that the directly measured data in both configurations are consistent based on comparisons against the results of direct numerical simulations. It was shown also, that notable uncertainties are introduced when extrapolations and density corrections are implemented in spherically expanding flames.

## Keywords:

Laminar Flames; Premixed Flames; Flame Propagation; Flame Kinetics.

## 1. Introduction

The laminar flame speed,  $S_u^o$ , is an important combustible mixture property and it is essential for the validation of chemical kinetics and the modeling of turbulent combustion. Furthermore,  $S_u^o$  is the only flame property that can be measured for pressures ranging from 0.1 to 50 atm, thus spanning all conditions of interest [1].

The relatively low sensitivity of  $S_u^o$  to chemical kinetics [2] prescribes experimental data with high accuracy and low uncertainty for validating and constraining the uncertainty of chemical models (e.g., [3]). Recent studies, however, have revealed that the uncertainty associated with the measurement of  $S_u^o$  can be large for flames of large molecular weight fuels [1], which would require modifications of rate constants beyond their uncertainty bounds [3]. The spherically expanding flame, SEF, and the counterflow flame, CFF, approaches are used extensively to measure  $S_u^o$  as they allow for the extraction of stretch effects from the raw data.

Traditionally,  $S_u^o$  measurements using SEF's include tracking the radius of an expanding flame,  $R_f$ , using optical techniques as a function of time,  $t$ , under constant pressure conditions (e.g., [4-13]). Then, the burned flame speed,  $S_b$  is obtained by differentiating  $R_f$  with respect to  $t$  on the assumption that the burned gas is stationary. The effect of stretch  $K \equiv \frac{2}{R_f} \frac{dR_f}{dt}$  is subtracted through extrapolation to zero stretch to obtain  $S_b^o$  followed by a density correction to obtain  $S_u^o$ .

Taylor [4] was the first to perform a linear extrapolation that has been used in many studies [5-11]. Kelley and Law [14] identified that for mixtures with non-unity Lewis number,  $Le$ , and Karlovitz numbers,  $Ka$ , relevant to experiments,  $S_b$  varies non-linearly with  $K$  and proposed a non-linear extrapolation equation, which was derived first by Ronney and Sivashinsky [15] for flames of mixtures sufficiently far from stoichiometry by assuming quasi-steady behavior, constant transport properties, and one-step reaction. Subsequently, Kelley et al. [16] relaxed the quasi-steady assumption and proposed an

improved non-linear extrapolation formula. Chen [17] and Kelley et al. [16] have tested the various extrapolation techniques using an asymptotic framework.

Recently, Jayachandran et al. [18] used detailed numerical simulation, DNS, for SEF's by computing both the  $S_b$  vs.  $K$  variation and  $S_u^o$ , and showed that the extrapolation equations of Law and coworkers [14,16] resulted in notable discrepancies with the known  $S_u^o$  value for mixtures with strong  $Le$  and differential diffusion effects. Chen [19] used DNS also to demonstrate that radiative heat loss from the burned gas results in a radially inward flow velocity, which causes a systematic decrease in  $S_b$  and thus  $S_b^o$ . Santner et al. [20] showed that this error increases for slowly propagating flames and also proposed a method of correction.

Jayachandran et al. [18] demonstrated that the error due to burned gas cooling due to radiation can be avoided by adopting the approach of Lecordier and coworkers [21,22]. The approach involves the tracking of a displacement speed relative to the fresh gases  $U_n \equiv S_b - U_g$ .  $U_g$  is defined as the maximum velocity upstream of the flame that is measured using high-speed particle image velocimetry (PIV), [Groot and De Goey Proc. Combust. Inst. (2002) 1445-1451]. Subsequently, this technique was improved and extended to liquid fuels by Renou and coworkers [23,24] to perform simultaneous high quality direct measurements of  $R_f$  and  $U_g$  as functions of time.

Law and coworkers [25-27] introduced the CFF approach for measuring  $S_u^o$ . The method involves the measurement of the axial velocity profile along the centerline, and the determination of a reference flame speed,  $S_{u,ref}$ , which is the minimum velocity just upstream of the flame. The characteristic stretch rate (strain rate),  $K$ , is defined as the maximum absolute value of the axial velocity gradient in the hydrodynamic zone. It was suggested first [25-27] that  $S_u^o$  is determined by linearly extrapolating  $S_{u,ref}$  to  $K = 0$ . Subsequently, Tien and Matalon [28] showed through asymptotic analysis that due to flow divergence and thermal dilatation the variation of  $S_{u,ref}$  with  $K$  is non-linear and proposed an equation to account for it.

Egolfopoulos and coworkers [29,30] introduced a computationally assisted approach that includes DNS of the experiment and detailed description of molecular transport and chemical kinetics, to extrapolate  $S_{u,\text{ref}}$  and obtain  $S_u^o$ . Notable discrepancies were identified under certain conditions when the results obtained by DNS and the equation of Tien and Matalon [28] were tested against a known answer.

It should be noted that  $S_u^o$  is not a directly measured but derived quantity and inconsistencies exist between data reported from CFF and SEF experiments. Those differences could be attributed to: (i) Experimental uncertainties related to the unburned mixture thermodynamic state and measuring approach among others; (ii) Radiative effects, non-negligible burned gas velocity, and/or density ratio assumption in SEF's; (iii) Extrapolation models and range of validity; and (iv) Potential geometrical effects.

The present investigation was the first step towards resolving some of these issues, and involved for the first time a combined experimental and computational approach in both SEF's and CFF's under the same conditions. The main innovation was that direct velocity measurements and direct numerical simulations (DNS) were carried out in both configurations. The specific goals of this study were: (1) To measure and compute propagation speeds in stretched flames. The thermodynamic conditions were chosen so that radiation had no measurable effect on the propagation of SEF's. Fuels with well-known combustion kinetics were used. Thus the consistency between measured and not extrapolated data obtained in both configurations could be evaluated indirectly through comparisons against reliable high-fidelity DNS results; (2) To quantify the bias introduced by extrapolation practices using both the experimental and computed results and comparing against the predicted 1D planar laminar flame speed that is the reference value. In doing so, it will be emphasized that a kinetic model could be validated with better accuracy using the stretched flame results both from experiments and DNS; and (3) To compare the  $S_u^o$  results obtained in SEF's using the variations of both  $S_b$  and  $U_n$  with the stretch rate.

## 2. Experimental approach

### 2.1. Spherically expanding flames

The apparatus and the post-processing method are described in detail in Refs. 23 and 24, and are briefly discussed below. Experiments are conducted in a high-pressure and high-temperature stainless steel spherical vessel with an inner radius of 85 mm. Mass flow rates of ethylene, oxygen and nitrogen are controlled by thermal mass flow meters (Bronkhorst). *n*-C<sub>7</sub>H<sub>16</sub> is vaporized in a controlled evaporator mixer (Bronkhorst) and injected into the vessel through heated lines. A Coriolis flow meter controls the liquid quantity to be vaporized. To ensure no re-condensation, the complete setup (lines and the combustion vessel) is heated up to 373 K. Before each set of measurements, the thermal mass flow meters are checked to avoid any systematic bias, using two different calibration systems based on two different physical principles (Coriolis mass flow meter Emerson CMFS010 and volumetric system BIOS Definer 220).

The accuracy of  $\phi$  is given by  $\frac{\Delta\phi}{\phi} = \sqrt{\left(\sum_i \frac{\Delta Q_i}{Q_i}\right)}$  where  $\Delta Q_i = 0.5\% \text{ Reading} + 0.1\% \text{ Full scale}$  is the manufacturer uncertainty of the thermal mass flow meter. The vessel is continuously flow fed with the mixture to achieve perfect mixture homogeneity within the combustion chamber. The pressure is measured with a piezoelectric sensor and kept constant by a control valve. Once both the mixture composition and the desired thermodynamic conditions are reached, the chamber is isolated using two pneumatic valves. The combustible mixture is spark-ignited at the center of the chamber by two tungsten electrodes separated by a 1.1 mm gap. Minimum energy is adjusted to limit ignition disturbances.  $S_b$  and  $U_g$  are obtained from high-speed laser tomography recordings, by using the new PIV algorithm presented in [23]. The chamber is seeded with silicone oil droplets (Rhodorsil), which vaporize at an isotherm of about 580 K. This boiling point temperature is high enough for the seeding droplets to exist well into the preheat zone, allowing for the determination of  $U_g$ . The effects of seeding on the flame dynamics, e.g. chemical and sensible enthalpy and re-absorption of radiative energy, have

been checked by performing shadowgraph measurements with and without seeding in the facility of Orléans [31], and no measurable effect was identified in a spherical chamber. From the tomographic measurements, both the time evolution of the flame radius  $R_f$  and spatial fresh gas velocity profiles can be obtained.  $S_b$  is determined through  $S_b = f'(t)$  where  $f(t)$  is obtained by a localized quadratic fitting of radius as a function of time. As mentioned earlier, the displacement speed is computed as  $U_n \equiv S_b - U_g$ .

All measurements were performed for  $0.7 \leq \phi \leq 1.4$  and  $p = 0.1$  MPa, and  $T_u = 298$  K for  $C_2H_4/(0.167 O_2 + 0.833 N_2)$  mixtures, and  $T_u = 373$  K for  $n-C_7H_{16}/air$  mixtures. The oxidizer was diluted for  $C_2H_4$  flames, in order to reduce the propagation rates to values similar to those of  $n$ -alkane/air flames and thus reduce experimental uncertainties. For each condition, 5 trials are performed to highlight the high level of repeatability of the measurements.

## 2.2. Counterflow flames

The experiments were carried out using the counterflow configuration [25,29,30]. The burner diameter and separation distance are 14 mm. All gaseous flow rates are metered using sonic nozzles. A high-precision pump, with a reported flow rate accuracy of  $\pm 0.5\%$ , is used to inject liquid fuel and a glass nebulizer is used to generate micron-size liquid fuel droplets which are mixed with hot air to achieve complete vaporization [30]. Uncertainty in  $\phi$  is no larger than 0.5%. A K-type thermocouple is used to monitor  $T_u$  at the center of the burner exit. The axial flow velocities were determined along the centerline using PIV [30], with submicron silicon oil droplets as flow tracers, to determine  $S_{u,ref}$  and  $K$ .

All measurements were performed at  $p = 1$  atm (0.101325 MPa), while all other conditions were identical to those used in SEF's.

### 3. Modeling approach

#### 3.1. Planar flames

$S_u^o$ 's are computed using the Premix code [32] that has been modified to include Soret effect and the optically thin model (OTM) for radiation from CH<sub>4</sub>, CO, CO<sub>2</sub>, and H<sub>2</sub>O [33]. CFF's flames are simulated using a modified version of an opposed-jet code [34,35]. Both codes are integrated with the Chemkin [36] and the Sandia transport [37] subroutine libraries. The USC Mech II kinetic model [38] was used for the C<sub>2</sub>H<sub>4</sub> flame simulations. For modeling *n*-C<sub>7</sub>H<sub>16</sub> flames, the JetSurF 1.0 [39] model was reduced to 100 species and 803 reactions using DRG [40].

#### 3.2. Spherically expanding flames

The recently developed transient one-dimensional reacting flow code (TORC) [18], using the Premix code [32] as framework, is utilized to model SEF's. High fidelity time integration of the spatially discretized conservation equations for mass, species' mass fractions, and energy is carried out using a new version of DASSL [41] solver, which implements a backward-difference formula (BDF) with adaptive time step and order control. An adaptive grid methodology was utilized to improve computational efficiency.

Adiabatic (ADB) and non-adiabatic (OTM) simulations were performed in a domain of size 25 cm, in order to assess potential radiation effects. A hot pocket of burned gas of radius 1.8 mm surrounded by the unburned mixture was used as an initial condition that led to ignition.  $R_f$  was identified as the 580 K isotherm, which is the boiling point of the silicon oil droplets used as tracer particles in the experiments.  $S_b$  and  $U_g$  were derived readily from the solutions.

## 4. Results and discussion

### 4.1 Direct measurements and simulations

Figure 1 and 2 depict the directly measured  $S_b$  and  $U_g$  from SEF's and  $S_{u,ref}$  from CFF's along with the corresponding DNS results at various  $\phi$ 's for  $C_2H_4$  and  $n-C_7H_{16}$  flames respectively.

SEF's were modeled using both ADB and OTM approaches and results show that under the present conditions radiation does not have a significant effect on either  $S_b$  or  $U_g$  for these relatively fast flames. CFF's were modeled using the OTM approach but the results obtained with the ADB are known to be indistinguishable from those obtained with OTM for non near-limit flames [33]. As mentioned in the Introduction, the choice of conditions was made to avoid complications stemming from radiation effects. However, if radiation effects were notable for SEF's, the DNS results could be compared only with the experimental  $U_n$  whose values are insensitive to the presence of radiation [18]. Additionally, it would not be possible to derive any information regarding  $S_b$  whose value depends directly on the burned gases velocity, and it is used as the main measurable quantity in the vast majority of SEF experiments.

The experimental and computed  $S_b$ ,  $U_g$ , and  $S_{u,ref}$  appear to be in good agreement. As expected,  $U_g$  and  $S_{u,ref}$  that are measured using PIV, exhibit a larger scatter compared to  $S_b$ . The difference on a percentage basis of the experimental  $S_b$ ,  $U_g$ ,  $U_n$ , and  $S_{u,ref}$  from the corresponding DNS results were computed. For each property and  $\phi$ , a mean difference and the corresponding standard deviation over the entire range of stretch rates was calculated, and Fig. 3 depicts the results as function of  $\phi$  for both  $C_2H_4$  and  $n-C_7H_{16}$  flames. First, it is interesting to note the consistency with which the model under-predicts or over-predicts the two different SEF measured values ( $S_b$  and  $U_g$ ), which were obtained by completely different approaches. Furthermore Second, the results show that direct measurements obtained in two completely different experimental systems are in close agreement with those obtained from the respective DNS, with most cases being within 4%. This is an important point as it

demonstrates that within the experimental uncertainty, the two approaches for measuring  $S_u^o$  are consistent with each other and that they provide very similar information. This conclusion was made possible simple because the directly measured properties were compared indirectly with each other through accurately performed DNS, without complications introduced by uncertainties associated with extrapolations. It is of interest to note also, that while  $U_n$  appears to have a larger standard deviation among all properties, being the difference of two much larger values, it exhibits on the average very similar differences from the DNS results as all other properties.

#### ***4.2 Extrapolation uncertainties***

~~The deviations of the  $S_u^o$  values, obtained from stretched SEF flame DNS results, from the corresponding stretch free values computed using Premix [32] were determined.~~

The SEF DNS results in the range  $1 \text{ cm} \leq R_f \leq 2 \text{ cm}$  were treated as “data,” within a  $R_f$  range for which data are typically obtained in experiments . Linear [4] and non-linear [16] extrapolations together with density corrections were utilized to obtain  $S_u^o$  from the flame radius as a function of time “data”.  $S_u^o$ ’s were also extracted from the  $U_n$  values applying the method adopted by Varea et al. [23] in which the non-linear equation of Kelley et al. [14] was used. ~~The error was calculated then as the difference between  $S_u^o$  obtained using either type of extrapolation, and  $S_u^o$  that is known as its value can be computed using the Premix code [32].~~ The DNS-based extrapolation error, which is calculated as the difference between the  $S_u^o$  value extracted from stretched DNS results employing extrapolations and the  $S_u^o$  value that is known as it can be computed using Premix [32], is shown in Fig. 4 as function of  $\phi$  for both  $\text{C}_2\text{H}_4$  and  $n\text{-C}_7\text{H}_{16}$  flames.

It is seen that for  $C_2H_4$  flames, the extrapolation deviations when  $S_b$  information is used are considerably small except for near stoichiometric conditions where predictions from both methods are at most 4% lower than the correct value. It is also of interest to note that for most  $\phi$ 's linear extrapolations reproduce closely the correct value of  $S_b^o$ , while the non-linear ones result in lower values. This is expected as  $C_2H_4$ ,  $N_2$ , and  $O_2$  have similar diffusivities so that  $Le$  and differential diffusion effects are absent and the linear  $S_b$  vs.  $K$  behavior is warranted [18].

In the case of  $n-C_7H_{16}$  flames, non-linear extrapolations using  $S_b$  data under predict the correct value for  $\phi = 0.7$  by 5%, whereas for  $\phi = 1.4$  both linear and non-linear extrapolations over-predict  $S_b^o$  by about 5%. Similar to  $C_2H_4$  flames, linear extrapolation reproduces very closely the correct value for  $\phi = 0.7$  that is reasonable as for this  $Le > 1$  mixture a near-linear  $S_b$  vs.  $K$  behavior is expected [18]. It was found also that for  $\phi = 0.7$ ,  $S_b$  decreases with  $K$  while for  $\phi = 1.4$  it increases. For  $\phi = 0.7$ ,  $Le > 1$  and as  $K$  increases the loss of heat from the reaction zone cannot be balanced by gain of fuel resulting in the reduction of the overall reaction rate [42]. The behavior for  $\phi = 1.4$  cannot be explained based on a  $Le$  argument as  $Le \approx 1$  based on  $O_2$  that is the deficient reactant. On the other hand, considering the reactant differential diffusion given that the diffusivity of  $O_2$  is greater than  $n-C_7H_{16}$ , increasing  $K$  results in progressively more stoichiometric  $\phi$  within the flame zone that tends to increase the overall reaction rate [18].

For  $C_2H_4$  and  $n-C_7H_{16}$  flames, non-linear extrapolation of  $U_n$  using the equation for unburned (upstream) flame speed from Ref. 14 results in a consistent over prediction of  $S_u^o$  by more than 5%.  $U_n$  is affected by thermal dilation and geometry [18], and the extrapolation formula does not account for these effects.

The effect of the data range was considered as well by increasing it by a factor of five. Using DNS results "data" in the range  $1 \text{ cm} \leq R_f \leq 6 \text{ cm}$  to extrapolate, results in considerably improved prediction

of both  $S_u^o$  and  $S_b^o$  in most majority of cases as shown in Fig. 4 as well. However, for the  $\phi = 0.7, 1.1$  and  $1.3$  cases an increase in extrapolation error is noticed when the non-linear equation to obtain  $S_b^o$  is used which is indicative of the fact that asymptotic equations are unable to capture the flame dynamics. Thus, either precaution has to be taken when using a large experimental chamber to extend the range of experimental data. Furthermore, utilizing data at smaller radii to increase data range may result in errors from ignition related effects and, the existing extrapolation formulas may not be reliable at very high stretch rates.

~~would not or extending, for a given chamber, the range of data to smaller flame radii could reduce significantly the extrapolation uncertainties. However, at smaller flame radii there may be ignition-related effects and due to the very high stretch rates the existing extrapolation formulas may not be reliable.~~

The deviations of the  $S_u^o$  values obtained through extrapolations using experimental data from the  $S_u^o$  values obtained through 1D planar computations were determined. The CFF extrapolated values were corrected to 0.1 MPa for consistency. The results are shown in Fig. 5 as function of  $\phi$  for both  $C_2H_4$  and  $n-C_7H_{16}$  flames. The deviations for the  $U_n$  extrapolated values are 5% or greater for most cases. In the case of  $C_2H_4$  flames, the deviations are at most 5% when CFF data are used for  $\phi = 0.7$  and  $1.4$ , for which flames are weaker and slower. For  $n-C_7H_{16}$  flames, the deviation for  $\phi = 0.7$  is nearly 15% for  $S_b^o$ .

A straightforward explanation of the results of Fig. 5 cannot be derived readily. Experimental measurements have inherent uncertainties, on which however one needs to superimpose uncertainties associated with extrapolation formulas to determine  $S_u^o$  that may or may not be able to capture the stretch effects under all conditions. It is noted however that the deviations from computed values of  $S_u^o$  are substantially different compared to those reported in Fig. 3, in which direct measurements and

simulations were compared especially for SEF's for which existing extrapolation [14,16] equations were used. Nevertheless, the deviation of the values obtained by DNS-assisted extrapolation of CFF data is consistent with the corresponding values in Fig. 3.

For SEF's, the previously mentioned inconsistencies will be augmented further if radiation induced flow [18] is neglected for flame conditions in which the effect is significant. Additionally, a major issue could be raised regarding the validity of the density correction approach that is based on the assumption of a single density value for the burned gases. It has been shown [18,20] that due to radiation there is a continuous variation of density throughout the burned gas region.

## 5. Concluding remarks

This is the first study aiming to consolidate and compare quantitatively data obtained in spherically expanding and counterflow flames using direct measurements as well as direct numerical simulations of ethylene and *n*-heptane flames. In both configurations, particle image velocimetry was used to determine the velocity fields and derive thus directly the physical quantities of relevance to the determination of laminar flame speeds. The simulations included the use of detailed description of chemical kinetics and molecular transport, and accurate time stepping in modeling spherically expanding flames

Considering only directly measured or directly computed quantities, uncertainties associated with extrapolations and/or density corrections for the case of spherically expanding flames are eliminated. The consistency between the two configurations was confirmed as in both cases the data were predicted closely by the numerical simulations within their inherent uncertainty. However, upon introducing linear and non-linear extrapolations as well as density corrections, the uncertainty increases. It was found also that under certain conditions non-linear extrapolations for spherically expanding flames are not reproducing known values at zero stretch, failing to capture the response of the flame to stretch. Typically, such formulas are derived based on simplified assumptions and while elegant and insightful they may not be appropriate for deriving experimental data of high fidelity against which kinetic rate parameters will be validated.

## Acknowledgements

At USC, the work was supported as part of the CEFRC, an Energy Frontier Research Center funded by the U.S. Department of Energy, Office of Science, and Office of Basic Energy Sciences under Award Number DE-SC0001198. At CNRS and Université d'Orléans, the work was supported by the European Regional Development Fund under Grant Interreg IV E3C3.

## References

- [1] F.N. Egolfopoulos, N. Hansen, Y. Ju, K. Kohse-Höinghaus, C.K. Law, F. Qi, "Recent advances and challenges in combustion chemistry: laminar flame experiments," submitted to Progress in Energy and Combustion Science.
- [2] A.T. Holley, X.Q. You, E. Dames, H. Wang, F.N. Egolfopoulos, Proc. Combust. Inst. 32 (2009) 1157-1163.
- [3] D.A. Sheen, H. Wang, Combust. Flame 158 (2011) 2358-2374.
- [4] S.C. Taylor, Burning Velocity and Influence of Flame Stretch, Ph.D. Thesis, University of Leeds, 1991.
- [5] K.T. Aung, M.I. Hassan, G.M. Faeth, Combust. Flame 109 (1997) 1-24.
- [6] S.D. Tse, D.L. Zhu, C.K. Law, Proc. Combust. Inst. 28 (2000) 1793-1800.
- [7] O.C. Kwon, G.M. Faeth, Combust. Flame 124 (2001) 590-610.
- [8] N. Lamoureux, N. Djebaili-Chaumeix, C.-E. Paillard, Exp. Therm. Fluid Sci. 27 (2003) 385-393.
- [9] Z. Huang, Y. Zhang, K. Zeng, B. Liu, Q. Wang, D. Jiang, Combust. Flame 146 (2006) 302-211.
- [10] C. Tang, Z. Huang, C. Jin, J. He, J. Wang, X. Wang, H. Miao, Int. J. Hydrogen Energy 33 (2008) 4906-4914.
- [11] E. Hu, Z. Huang, J. He, C. Jin, J. Zheng, Int. J. Hydrogen Energy 34 (2009) 4876-4888.
- [12] G.E. Andrews, D. Bradley, Combust. Flame 19 (1972) 275-288.
- [13] X. Qin, Y. Ju, Proc. Combust. Inst. 30 (2005) 233-240.
- [14] A.P. Kelley, C.K. Law, Combust. Flame 156 (2009) 1844-1851.
- [15] P.D. Ronney, G.I. Sivashinsky, SIAM J. Appl. Math. 49 (1989) 1029-1046.
- [16] A.P. Kelley, J.K. Bechtold, C.K. Law, J. Fluid Mech. 691 (2012) 26-51.
- [17] Z. Chen, Combust. Flame 158 (2011) 291-300.
- [18] J. Jayachandran, R. Zhao, F.N. Egolfopoulos, "Determination of laminar flame speeds using stagnation and spherically expanding flames: molecular transport and radiation effects," submitted to Combustion and Flame.
- [19] Z. Chen, Combust. Flame 157 (2010) 2267-2276.
- [20] J. Santner, F.M. Haas, Y. Ju, F.L. Dryer, Combust. Flame 161 (2014) 147-153.
- [21] B. Lecordier. Etude de l'interaction de la propagation d'une flamme de prémélange avec le champ aérodynamique par association de la tomographie laser et de la PIV. PhD Thesis Report, Université de Rouen, France, 1997.
- [22] S. Balusamy, A. Cessou, B. Lecordier, Exp. Fluids 50 (2011) 1109-1121.

- [23] E. Varea, V. Modica, A. Vandel, B. Renou, *Combust. Flame* 159 (2012) 577-590.
- [24] E. Varea, V. Modica, B. Renou, A.M. Boukhalfa, *Proc. Combust. Inst.* 34 (2013) 735-744.
- [25] C.K. Wu, C.K. Law, *Proc. Combust. Inst.* 20 (1985) 1941–1949.
- [26] C.K. Law, D.L. Zhu, G. Yu, *Proc. Combust. Inst.* 21 (1988) 1419–1426.
- [27] F.N. Egolfopoulos, P. Cho, C.K. Law, *Combust. Flame* 76 (1989) 375-391.
- [28] J.H. Tien, M. Matalon, *Combust. Flame* 84 (1991) 238-248.
- [29] Y.L. Wang, A.T. Holley, C. Ji, F.N. Egolfopoulos, T.T. Tsotsis, H. Curran, *Proc. Combust. Inst.* 32 (2009) 1035–1042.
- [30] C. Ji, E. Dames, Y.L. Wang, H. Wang, F.N. Egolfopoulos, *Combust. Flame* 157 (2010) 277-287.
- [31] F. Halter, T. Tahtouh, C. Mounaim-Roussele, *Combust. Flame* 157 (2010) 1825-1832.
- [32] R.J. Kee, J.F. Grcar, M.D. Smooke, J.A. Miller, *Premix: A FORTRAN Program for Modeling Steady Laminar One-dimensional Premixed Flames*, Sandia Report, SAND85- 8240, Sandia National Laboratories, 1985.
- [33] F.N. Egolfopoulos, *Proc. Combust. Inst.* 25 (1994) 1375–1381.
- [34] F.N. Egolfopoulos, C.S. Campbell, *J. Fluid Mech.* 318 (1996) 1–29.
- [35] R.J. Kee, J.A. Miller, G.H. Evans, G. Dixon-Lewis, *Proc. Combust. Inst.* 22 (1988) 1479–1494.
- [36] R.J. Kee, F.M. Rupley, J.A. Miller, *Chemkin-II: A Fortran Chemical Kinetics Package for the Analysis of Gas-Phase Chemical Kinetics*, Report No. SAND89- 8009, Sandia National Laboratories, 1989.
- [37] R.J. Kee, J. Warnatz, J.A. Miller, *A FORTRAN Computer Code Package for the Evaluation of Gas-Phase Viscosities, Conductivities and Diffusion Coefficients*, Report No. SAND83-8209, Sandia National Laboratories, 1983.
- [38] H. Wang, X. You, A. V. Joshi, Scott G. Davis, A. Laskin, F.N. Egolfopoulos C. K. Law, USC-Mech Version II. High-Temperature Combustion Reaction Model of H<sub>2</sub>/CO/C<sub>1</sub>-C<sub>4</sub> Compounds. [http://ignis.usc.edu/USC\\_Mech\\_II.htm](http://ignis.usc.edu/USC_Mech_II.htm).
- [39] B. Sirjean, E. Dames, D. A. Sheen, X. You, C. Sung, A. T. Holley, F. N. Egolfopoulos, H. Wang, S. S. Vasu, D. F. Davidson, R. K. Hanson, H. Pitsch, C. T. Bowman, A. Kelley, C. K. Law, W. Tsang, N. P. Cernansky, D. L. Miller, A. Violi, R. P. Lindstedt, “A High-Temperature Chemical Kinetic Model of *n*-Alkane Oxidation, JetSurF Version 1.0,” <http://melchior.usc.edu/JetSurF/JetSurF1.0/Index.html>.
- [40] T. Lu, C.K. Law, *Proc. Combust. Inst.* 30 (2005) 1333–1341.

- [41] L.R. Petzold, A Description of DASSL: A Differential/Algebraic System Solver, in Scientific Computing, R.S. Stepleman et al. (Eds.), North-Holland, Amsterdam, 1983, pp. 65-68.
- [42] C.K. Law, Combustion Physics, Cambridge University Press, 2008.

### Figure captions:

- Figure 1.** Experimental and computed  $S_b$  (top),  $U_g$  (center), and  $S_{u,ref}$  (bottom) as functions of stretch rate for  $C_2H_4$  flames. Symbols: experimental data; Thick lines: ADB simulations for SEF's and CFF's; Dotted lines: OTM simulations for SEF's only.
- Figure 2.** Experimental and computed  $S_b$  (top),  $U_g$  (center), and  $S_{u,ref}$  (bottom) as functions of stretch rate for  $n-C_7H_{16}$  flames. Symbols: experimental data; Thick lines: ADB simulations for SEF's and CFF's; Dotted lines: OTM simulations for SEF's only.
- Figure 3.** Mean difference and standard deviation of experimentally measured  $S_b$ ,  $U_g$ ,  $U_n$ , and  $S_{u,ref}$  from the computed values, as a function of equivalence ratio.
- Figure 4.** Deviation of DNS-based extrapolated  $S_u^o$  values from computed ones as function of equivalence ratio for SEF's using two different ranges of flame radii for extrapolation:  $1\text{ cm} \leq R_f \leq 2\text{ cm}$  (left) and  $1\text{ cm} \leq R_f \leq 6\text{ cm}$  (right). Error values represented by symbols: (×) linear method for  $S_b$ ; (□) non-linear method for  $S_b$ ; and (Δ) non-linear method for  $U_n$ .
- Figure 5.** Deviation of experiment-based extrapolated  $S_u^o$  values from computed ones as function of equivalence ratio. Differences represented by symbols: (◇) non-linear method for  $S_{u,ref}$  from CFF's; (×) linear method for  $S_b$ ; (□) non-linear method for  $S_b$ ; and (Δ) non-linear method for  $U_n$  from SEF's.

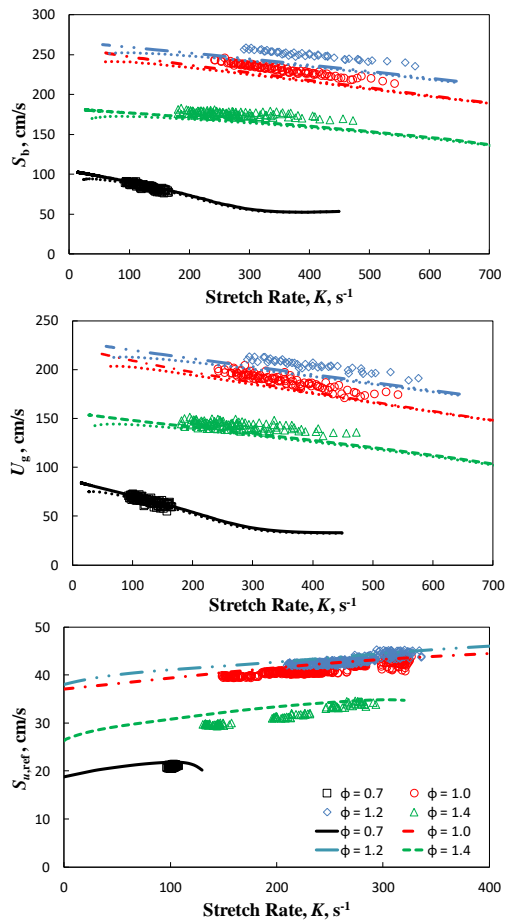


**Figure 1.** Experimental and computed  $S_b$  (top),  $U_g$  (center), and  $S_{u,ref}$  (bottom) as functions of stretch rate for  $C_2H_4$  flames. Symbols: experimental data; Thick lines: ADB simulations for SEF's and CFF's; Dotted lines: OTM simulations for SEF's only.

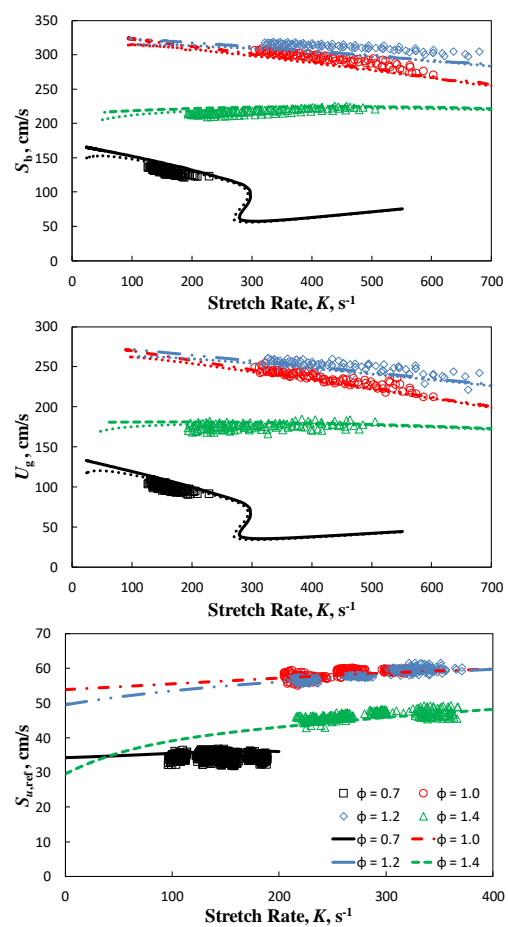


**Figure 2.** Experimental and computed  $S_b$  (top),  $U_g$  (center), and  $S_{u,\text{ref}}$  (bottom) as functions of stretch rate for  $n\text{-C}_7\text{H}_{16}$  flames. Symbols: experimental data; Thick lines: ADB simulations for SEF's and CFF's; Dotted lines: OTM simulations for SEF's only.

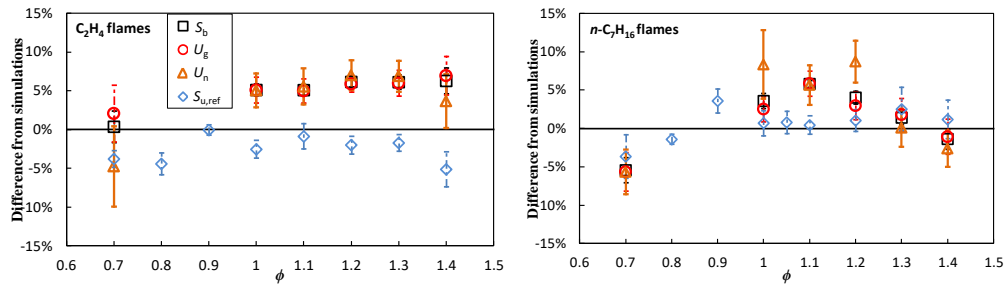


**Figure 3.** Mean difference and standard deviation of experimentally measured  $S_b$ ,  $U_g$ ,  $U_n$ , and  $S_{u,ref}$  from the computed values, as a function of equivalence ratio.

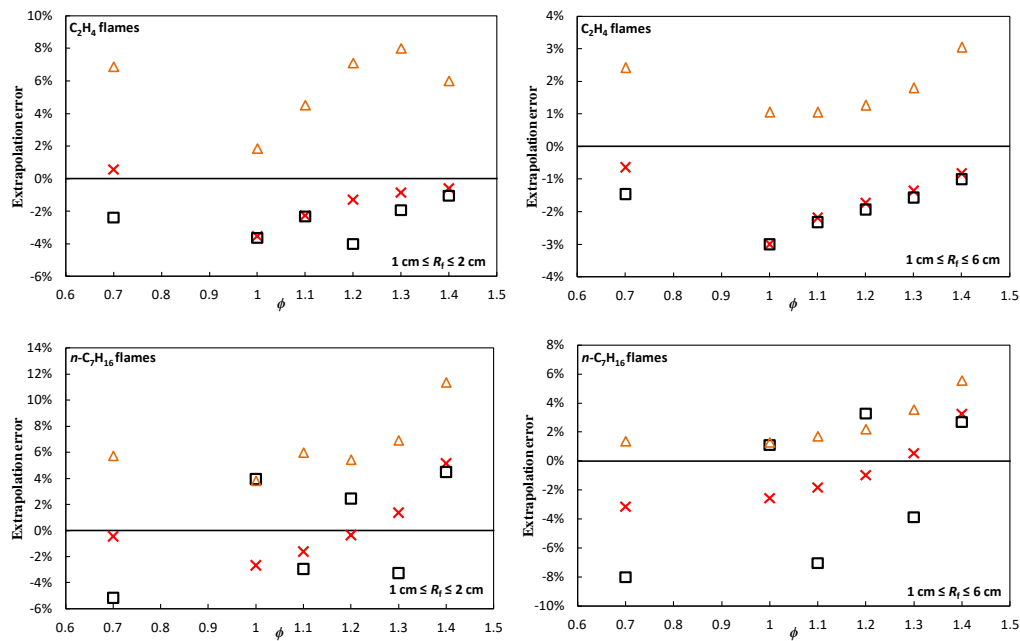


**Figure 4.** Deviation of DNS-based extrapolated  $S_u^o$  values from computed ones as function of equivalence ratio for SEF's using two different ranges of flame radii for extrapolation:  $1 \text{ cm} \leq R_f \leq 2 \text{ cm}$  (left) and  $1 \text{ cm} \leq R_f \leq 6 \text{ cm}$  (right). Error values represented by symbols: ( $\times$ ) linear method for  $S_b$ ; ( $\square$ ) non-linear method for  $S_b$ ; and ( $\triangle$ ) non-linear method for  $U_n$ .

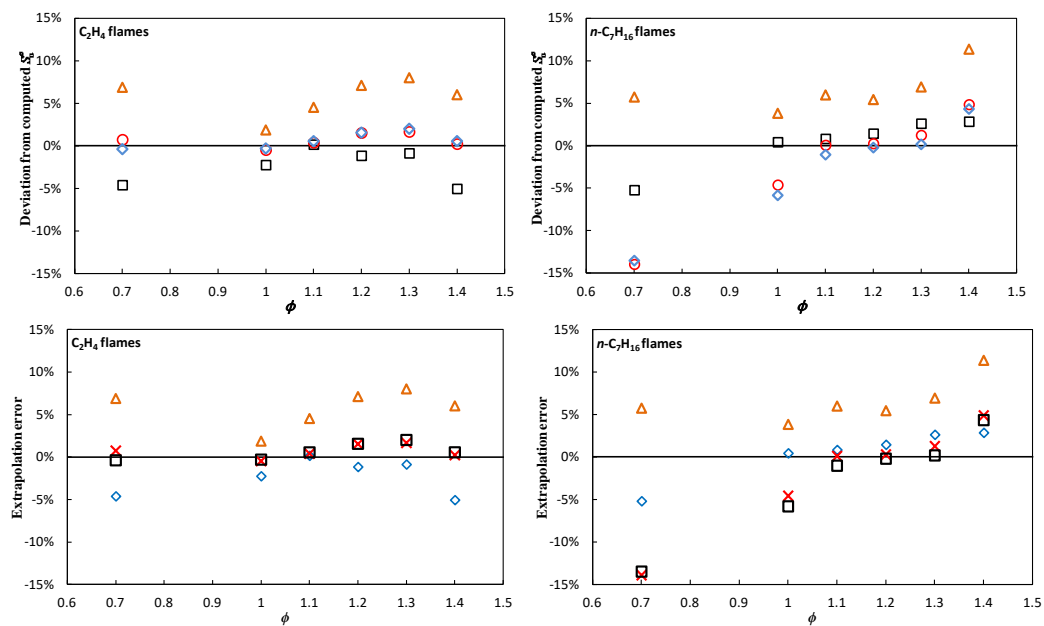


**Figure 5.** Deviation of experiment-based extrapolated  $S_u^o$  values from computed ones as function of equivalence ratio. Differences represented by symbols: (◇) non-linear method for  $S_{u,ref}$  from CFF's; (×) linear method for  $S_b$ ; (□) non-linear method for  $S_b$ ; and (△) non-linear method for  $U_n$  from SEF's.